Exploring the influence of S. cerevisiae mannoproteins on wine astringency and color: Impact of their polysaccharide part

Saul Assunção Bicca, Céline Poncet-Legrand, Stéphanie Roi, Julie Mekoue, Thierry Doco, Aude Vernhet

Exploring the influence of *S. cerevisiae* mannoproteins on wine astringency and color: impact of their polysaccharide part

Saul ASSUNÇÃO BICCA[a,b*], Céline PONCET-LEGRAND[a], Stéphanie ROI[a], Julie MEKOUE[b], Thierry DOCO[a] and Aude VERNHET[a]

[a] SPO Institut Agro, INRAE, Univ Montpellier, Montpellier, France.

[b]Lallemand, SAS, 19 rue des Briquetiers, BP 59, 31702 Blagnac, France.

* Corresponding author

Saul Assunção Bicca, Institut Agro - Montpellier SupAgro, UMR 1083 Sciences pour l'œnologie (SPO), bât. 28, 2 place Viala, F-34060 Montpellier, France.

Phone: +33 (0) 4 99 61 27 58

Email addresses: saul.assuncao@supagro.fr

celine.poncet-legrand@inrae.fr

jmekoue@lallemand.com

thierry.doco@inrae.fr

aude.vernhet@supagro.fr

Abstract

The impact of the polysaccharide moiety of mannoproteins (MPs) on the color and astringency of red wines was studied respectively through spectrophotometry and their impact on tannin interactions with BSA. To this end, MPs with conserved native structures from four different *Saccharomyces cerevisiae* strains were used: a Wild-Type strain (BY4742, WT) taken as reference, mutants ΔMnn4 (with no mannosyl-phosphorylation) and ΔMnn2 (linear N-glycosylation backbone), and a commercial enological strain. MPs affected tannin-BSA interactions by delaying aggregation kinetics. To achieve it, a well-balanced density/compactness of the polysaccharide moiety of MPs was a key factor. MP-WT and MP-Mnn2 acted as weak copigments and induced a slight increase in the absorbance of Malvidin-3-*O*-Glucoside. The same MPs also promoted a synergistic effect during the copigmentation of Quercetin-3-*O*-Glucoside with Malvidin-3-*O*-Glucoside. The intensity of these hyperchromic effects was related to the accessibility of anthocyanins to negatively charged mannosyl-phosphate groups within the polysaccharide moiety.

Keywords: Mannoproteins; Physico-chemical interactions; Astringency; Wine color; Copigmentation.

1 Introduction

Color and astringency are essential organoleptic characteristics of red wines that determine their quality, price, and reputation among consumers and winemakers. Both characteristics are directly linked to wine composition in polyphenols. The wine color is dependent on its composition in anthocyanins extracted from the grape skin during maceration and derived pigments formed during winemaking and aging through different reaction pathways (Cheynier et al., 2006; De Freitas & Mateus, 2011; Fulcrand, Dueñas, Salas, & Cheynier, 2006). Astringency is related to the presence of tannins and to their capacity to interact with and precipitate salivary proline-rich proteins (PRPs) (Bate-Smith, 1973). Besides the polyphenol composition of red wines, many other factors affect these characteristics (González-Muñoz et al., 2022). Among them are the physico-chemical interactions that may occur between polyphenols and other wine components.

Anthocyanins in red wines (pH 3-4) are present in different forms: the red-colored flavylium cation, the colorless hydrated hemiacetal form, and the deprotonated violet quinoidal base (Raymond Brouillard & Dubois, 1977), all the above being themselves in equilibrium with the chalcone forms characterized by a yellow color. Their physico-chemical interactions with other anthocyanins (self-association) or with other phenolic compounds (intra or intermolecular copigmentation) lead to the formation of molecular complexes that protect and stabilize flavylium species. These interactions are related to van der Waals forces between the planar polarizable nuclei (π-π stacking) of anthocyanin and phenolic co-pigment. Self-association and copigmentation also influence the optical properties of the anthocyanins inducing an increase in absorbance (hyperchromic effect) and/or a shift of the maximum absorption (bathochromic effect). Several studies underline the impact of the anthocyanin and copigment structures on the formation of molecular complexes and their consequences on wine color (Trouillas et al.,

2016). An impact on anthocyanin color has also been evidenced for polysaccharides, especially pectic polysaccharides (Fernandes, Brás, Oliveira, Mateus, & De Freitas, 2016; Gonçalves, Rocha, & Coimbra, 2012; Lin, Fischer, & Wicker, 2016; Padayachee et al., 2012). The capacity of these non-phenolic copigments to modulate the color properties of anthocyanins is mainly attributed to interactions between the flavylium cation and the linear homogalacturonan chains of pectins. These interactions depend on both the degree of esterification of the uronic acids (Fernandes et al., 2020; Trouillas et al., 2016) and the presence of side chains of neutral sugars (Fernandes et al., 2021). While pectins play an important role in stabilizing the color of anthocyanins in several food matrixes, homogalacturonan chains are hydrolyzed during wine processing by pectinases (pectin-methylesterases, polygalacturonases, pectin lyases, etc.) so that linear pectins (or homogalacturonans) are not expected to have such a high impact.

Astringency is a complex tactile sensation of drying and puckering in mouth, caused by a loss of lubricity in oral saliva. In red wines, it is attributed to physico-chemical interactions between polymeric polyphenols and salivary proteins, causing their aggregation and precipitation (Cheynier, 2012). While tannins play an essential role in the astringency of wines, other compounds in the matrix can modulate it by their ability to either generate analogous sensations or interfere with tannin-protein interactions. Different studies have shown that polysaccharides, and in particular wine pectic polysaccharides, can interfere with tannin-protein interactions (Boulet et al., 2016; Carvalho, Póvoas, Mateus, & De Freitas, 2006; Quijada-Morín, Williams, Rivas-Gonzalo, Doco, & Escribano-Bailón, 2014). Depending on the considered protein and polysaccharide, two kinds of mechanisms have been proposed to explain the impact of polysaccharides on protein-tannin interactions and their ability to modulate astringency: a) the formation of a ternary protein-polyphenol-polysaccharide system where the polysaccharide part would stabilize the colloidal aggregates formed by protein/polyphenol

interactions, and b) a competition between polysaccharide and protein for tannin binding (Brandão et al., 2017; Soares, Mateus, & de Freitas, 2012).

The impact of mannoproteins, one of the most important families of wine polysaccharides, on the color and astringency of red wines have been demonstrated respectively: through their capacity to stabilize colloidal coloring matter (Escot, Feuillat, Dulau, & Charpentier, 2001; Guadalupe, Martínez, & Ayestarán, 2010; Oyón-Ardoiz, Manjón, Escribano-Bailón, & García-Estévez, 2022), and through sensorial analysis (Manjón, Recio-Torrado, Ramos-Pineda, García-Estévez, & Escribano-Bailón, 2021; Rinaldi, Coppola, & Moio, 2019; Vidal et al., 2003; Wang et al., 2021). Although more recent studies elucidate the effect of commercial preparations of mannoproteins on tannin-protein interactions and in the particle sizes of aggregates formed, no advances were made in the interaction mechanisms that take place (Manjón et al., 2021; Wang et al., 2021). Regarding wine color, beyond their impact on colloidal stability of wines, few studies have taken interest in the potential interactions developed between mannoprotein and anthocyanins. Mannoproteins purified from red wine were capable of developing interactions with anthocyanins in model conditions, these interactions being higher for acylated forms (Gonçalves et al., 2018) whilst little is known about the nature of these interactions and their consequences at color-level.

Four mannoprotein pools were previously extracted and purified from different yeast strains and fully characterized (Assunção Bicca et al., 2022). One was extracted from a commercial enological strain, MP-Com, and presented a high mannose content and a compact and highly branched polysaccharide structure. Three others were extracted from a laboratory strain (wild-type, taken as reference) and two of its mutants, Mnn2 and Mnn4. From the mannoproteins extracted from the referential strain (MP-WT), MP-Mnn4 only differed by the absence of mannosyl-phosphate residues in the polysaccharide moiety, whereas MP-Mnn2 was characterized by the absence of ramification of its N-glycosylated chains (**Supplementary**

data, Figure S1). Furtherly, the interaction capacities of these mannoproteins when facing high aDP and galloylation level seed tannins were evaluated at a thermodynamic and colloidal levels. The structural differences in the polysaccharide structure among the four MP pools (molecular compactness, global net-charge, presence of mannosyl-phosphate groups, and the branching degree) resulted in no significant impact neither in the exothermic interactions ongoing nor in the size and polydispersity of the colloids formed between MPs and seed tannins.

Our aim in the present study was to further explore the impact of the mannoprotein structure, especially that of its polysaccharide part, on their ability to interfere in tannin-protein interactions and in color properties of anthocyanins in model conditions. The impact of mannoproteins on the interactions between proteins and tannins was studied using Bovine-Serum-Albumin (BSA) and purified red wine tannins. Although measuring the astringency potential of red wines without the need for sensory analyses is challenging, studies have shown good statistical correlations between astringency and protein-precipitation tests, in which the protein used was BSA (Boulet et al., 2016; Harbertson, Kilmister, Kelm, & Downey, 2014). Condensed tannins were isolated from red wines to avoid interference from other polyphenolic species and were used to consider the compositional and conformational modifications of tannins during winemaking and aging, which change their interaction capacities (McRae, Falconer, & Kennedy, 2010; Mekoue Nguela, Poncet-Legrand, Sieczkowski, & Vernhet, 2016). Meanwhile, interactions between malvidin-3-*O*-glucoside (Mal3glc) and mannoproteins were studied employing spectrophotometric measurements. Mal3glc was taken as standard due to the predominance of this form and its derivatives in grape berries and wines.

Our hypotheses are that mannoproteins may affect tannins-BSA interactions and the consequent aggregation related to astringency, and that this effect is dependent on the characteristics of the polysaccharide structure of mannoproteins. Concerning color, the

hypothesis is that the presence of mannosyl-phosphate groups may impact the interaction capacities of mannoproteins towards anthocyanins.

2 Materials and Methods

2.1 Mannoproteins

Mannoprotein pools used in the present study were extracted and purified from four different yeast strains: a commercial enological strain LMD47 provided by Lallemand SAS, a wild-type BY4742 strain (MATα; ura3Δ0; leu2Δ0; his3Δ1; lys2Δ0), and its mutants ΔMnn4 (MATα; ura3Δ0; leu2Δ0; his3Δ1; lys2Δ0; YKL201c::kanMX4) and ΔMnn2 (MATα; ura3Δ0; leu2Δ0; his3Δ1; lys2Δ0; YBR015c::kanMX4). The last three strains were obtained from EUROSCARF (European Saccharomyces Cerevisiae Archive for Functional Analysis). The methodology applied to obtain the mannoprotein pools from these strains (biomass production, enzymatic-extraction with β-glucanases, and purification steps) as well as their characterization were detailed previously (Assunção Bicca et al., 2022) and summarized in **Supplementary data, Table S1 and Figure S1**. The final mannoprotein pools were named after the yeast strains from which they were extracted: MP-Com, MP-WT, MP-Mnn4, and MP-Mnn2.

2.2 Malvidin-3-*O*-Glucoside and isoquercetin

The Malvidin-3-*O*-glucoside (purity of 95%) used was purchased from EXTRASYNTHESE (Lyon, France). Quercetin-3-*O*-glucoside was purchased from Sigma-Aldrich (Lyon, France).

2.3 Wine tannins

2.3.1 Tannin purification

Wine tannins were obtained from a Syrah red wine, produced through a thermovinification process at the Experimental Unit of Pech Rouge (INRAE, Gruissan, France). The whole polyphenol content was previously purified at the Laboratory (UMR SPO). Briefly, 10 L of wine were dealcoholized by evaporation under vacuum at low temperature (35 °C). The

resulting dealcoholized solution was mixed with 10 L vinyl-divinylbenzene Diaion resin (RELITE SP411) until complete polyphenol adsorption (followed by UV-visible spectrophotometry). The resin was washed several times with acidified water (0.05% trifluoroacetic acid, TFA) to remove non-phenolic compounds (sugars, organic acids, salts, polysaccharides, etc) until a value of 0 °Brix was obtained. Complex grape pectic polysaccharides such as RG II were then removed by washing the resin with 90/10/0.05 v/v water/ethanol/TFA. Polyphenol desorption was achieved by successive washings with 96/4/0.05 v/v ethanol/water/TFA, followed by UV-visible spectrophotometry. Ethanol was removed by evaporation under vacuum at a low temperature (35 °C). The polyphenol pool was freeze-dried and stored at -80 °C under argon atmosphere before use.

Fractioning of wine polyphenols was performed through affinity chromatography using a 200 mL bed-volume column packed with Fractogel® EMD Phenyl (S) (Millipore, France). Chromatographic process was assisted by an NGC Chromatographic System (BioRad, USA) equipped with diode array detectors (monitored wavelengths: 280, 320, 360, and 520 nm). Around 0.8 g of Syrah-wine polyphenols, dissolved in acidified water, were loaded into the column already equilibrated with the same eluent, and then washed with two bed-volumes of acidified water to ensure polyphenol adsorption to the resin. The release of three different polyphenol fractions was achieved with the following solvents: 50/50/0.05 v/v/v ethanol/water/TFA, 60/40/0.05 v/v/v ethanol/water/TFA, and 70/30/0.05 v/v/v acetone/water/TFA. The last eluted fraction represents the Syrah Wine Tannins (SWT) used. All fractions were concentrated under vacuum at low temperature (35 °C), freeze-dried, and stored at -80 ºC.

2.3.2 Tannin analysis

The absence of monomeric and oligomeric polyphenols in the wine-tannin fraction was assessed by HPLC-DAD (Kennedy & Jones, 2001) and HPSEC-DAD. For HPSEC-DAD

analysis, SWT was dissolved in a solution composed of 94% v/v N,N-dimethylmethanamide (DMF), 1% v/v acetic acid, 5% water, and 0.15 M of LiCl. The solution was injected into a 1260 Infinity II HPLC system (Agilent Technologies, Santa Clara, USA) equipped with: a vacuum degasser, an autosampler, an isocratic pump (1 $mL.min^{-1}$), a column heater (60 ^{o}C), and a diode array detector (280, 320, 360, and 520 nm), equipped with 3 Phenomenex Phenogel columns (300 mm x 7.8 mm, 5µm) with 10^6 Å, 10^3 Å, and 50 Å pore sizes, and a guard column (50 mm x 7.8 mm, 5 µm) of the same composition. Chromatographic analysis was performed with the OpenLab software. Most molecules were eluted at times between 22 and 27 minutes, with a maximum at 24.5 minutes, which corresponds to an average molecular weight of 2 800 $g.mol^{-1}$, which corresponds to a degree of polymerization of 9-10 on the basis of a calibration with standards (catechin and dimer B2) and apple tannins fractions of 1 735 and 11 561 $g.mol^{-1}$ (**Supplementary data, Figure S2**).

2.4 Interaction between BSA, mannoproteins, and wine tannins

2.4.1 Sample preparation

The impact of mannoproteins on the interactions between SWT and BSA was explored by Dynamic Light Scattering (DLS). All experiments were performed in a model wine solution composed of 2 $g.L^{-1}$ of tartaric acid, 12% v/v ethanol, 30 $mg.L^{-1}$ of sodium bisulfite, the pH (3.5) and the ionic strength (50 mM), the last two parameters of which were adjusted with 10^{-1} N NaOH and NaCl, respectively. The concentration of BSA and SWT were set at 0.05 and 0.2 $g.L^{-1}$, respectively. These concentrations were chosen so that interactions could be monitored by DLS for over an hour. Interaction assays with mannoproteins were carried out in two different ways: i) by mixing MP and SWT first, and then adding BSA after 2 hours for DLS analysis; ii) by mixing MP and BSA first, and then adding SWT after 2 hours for DLS analysis. MP/SWT and MP/BSA mixtures were also analyzed. Experiments were performed in triplicate

with MP concentrations at 1 and 0.5 $g.L^{-1}$. A final DLS measurement was performed after 24 h without re-suspending the precipitated colloids. Samples were then centrifuged for 15 min at 15 000 rpm after 48 h. In order to evaluate the tannin subfractions prioritized in these interactions, precipitates and aliquots of the supernatants were dried at low temperature (< 35 ºC) and the molecular size distribution of tannins was analyzed by HPSEC-DAD, as described before. Aliquots of the supernatants were also analyzed by absorbance measurements at 280 nm to determine the % of precipitated tannins. Absorbance measurements were performed with a UV-visible spectrophotometer (UV1900, Shimazu, Japan).

2.4.2 Dynamic Light Scattering

The influence of the different MPs in the interactions between SWT and BSA was followed during one hour by DLS measurements, carried out on a Malvern Zetasizer NanoZS (Malvern Instruments, Malvern, U.K.) equipped with a 4 mW He-Ne laser (633 nm), at an angle of 173° to the incident beam. Measurements were performed using a 1 cm pathway cuvette thermostat at 25 °C. The number of measurements, the attenuation level, and the measurement time were automatically set by the software and optimized for each sample analyzed. The hydrodynamic diameter of the particles in suspension was calculated using the Stokes-Einstein equation presented below (assuming a spherical form of the particles in suspension): $D(h)=kT/3\pi\eta D$, in which k, T, η, and D represent, respectively, the Boltzmann's constant, the absolute temperature, the dispersant dynamic viscosity (1.33 cP for 12 % ethanol v/v) and the diffusion coefficient. The last was determined by monitoring the time dependence of the scattered light and compiling an autocorrelation function G(t) of the dispersed species in the medium. The cumulant analysis was used to fit the autocorrelation curves, and to calculate the mean hydrodynamic diameter (D_{hS}) and the polydispersity index (PDI) of the dispersion.

2.5 Interactions between MPs and Malvidin-3-*O*-Glucoside

2.5.1 Titration associated with spectrophotometry analysis

The effect of MPs in the visible absorbance spectrum (400 - 650 nm) of Mal3glc was assessed through different titration methods. To this end, a given volume of titrant solution was added to a given sample, the solutions were homogenized, and the absorbance spectrum was recorded 5 min after. All samples were prepared in a model wine composed of 12% v/v ethanol/water and 2 $g.L^{-1}$ of tartaric acid, pH (3.5) and ionic strength (50 mM) adjusted with 0.1 M NaOH and NaCl solutions, respectively. No sodium bisulfite was used in these experiments. The absorbance spectra were measured with a SHIMADZU-UV1900 spectrophotometer. At pH 3.5, the maximum absorbance value for malvidin-3-*O*-Glucoside alone was observed at 525 nm. To avoid turbidity issues during the spectrophotometric measurements, mother solutions of each MP were centrifuged at 5 000 rpm/15 min before any sample preparation. All experiments were performed in triplicate at 25 ºC.

2.5.1.1 Effect of MPs on the absorbance spectrum of Mal3glc

In the first titration method, 2 mL samples of MPs (0.25 $g.L^{-1}$) plus Mal3glc (4.7 $x10^{-3}$ $g.L^{-1}$ or 9.45 $x10^{-3}$ mM) were titrated with 20 µL of a Mal3glc solution at 0.47 $g.L^{-1}$ (9.45 $x10^{-1}$ mM). The control samples had no MPs. Blank solutions of MPs at 0.25 $g.L^{-1}$ (with no Mal3Glc) had no absorbance within the visible spectrum range. Thirteen 20 µL additions were performed with this first titration method. Each addition was performed into the 5 samples simultaneously before measuring the absorbance spectra: control, MP-Com, MP-WT, MP-Mnn2, and MP-Mnn4.

In a second experiment, stock solutions of Mal3glc and mannoproteins were prepared in the model wine at twice the targeted final concentrations. Equal volumes of these stock solutions were mixed to achieve a final Mal3glc concentration of 46 $mg.L^{-1}$ (0.094 mM), and 2

different mannoprotein concentrations: 1 and 2 g.L^{-1}. All solutions were let to equilibrate 30 min before spectrophotometric measurements.

2.5.1.2 Effect of mannoproteins on malvidin-3-O-glucoside co-pigmentation with quercetin-3-O-glucoside

To explore the effect of the co-pigmentation of Mal3glc on its interaction with mannoproteins, (Mal3glc + MP) solutions were titrated with quercetin-3-*O*-glucoside (Qrc3glc). Samples at a 1 g.L^{-1} of MP and 57.8 mg.L^{-1} (0.117 mM) Mal3glc were titrated with a 0.5 g.L^{-1} (1.08 mM) solution of Qrc3glc. A control sample with no MPs was used. Additions were performed with a progressive increase of the solution volume: 50 µL twice, 100 µL twice, and 200 µL once. Five samples followed this titration simultaneously: control, MP-Com, MP-WT, MP-Mnn2, and MP-Mnn4.

3 Results and discussion

3.1 Kinetics of BSA, Syrah Wine Tannins, and Mannoproteins interactions

Interactions between mannoproteins, Syrah Wine Tannins (SWT), and Bovine serum albumin (BSA) were explored through DLS measurements. BSA and SWT concentrations (50 and 200 mg.L^{-1}, respectively) were chosen to limit the rate of aggregation so that it could be monitored by DLS. Aggregation was followed by changes in the average hydrodynamic diameter D_{hS}, Polydispersity Index, as well as in scattered intensity I_S. Both SWT and BSA samples had very low I_S values (lower than 500 kcps), associated with very low signal-to-noise ratios. No correlation function could be measured. Mixing SWT and BSA led to immediate and strong increases in I_S, related to the formation of aggregates with measurable D_{hS} (**Figure 1**). At the end of the first DLS measurement (2-4 min after mixing SWT and BSA), I_S ranged between 15 000 to 20 000 kcps and D_{hS} values between 650 to 700 nm. D_{hS} values then continued to grow until a plateau value between 2 500 and 3 000 nm, reached after 50 min. The

polydispersity remained relatively low (0.385 ± 0.130), indicating that the particle size evolved homogenously. In parallel, I_S remained stable. This indicated that particle growth was mainly related to the enlarged co-aggregation of previously formed BSA-SWT aggregates. After 1 hour, a gradual decrease of I_S indicated sedimentation of the micron-sized aggregates. Phase separation was observed after 24 h.

Interaction experiments between BSA and SWT were repeated in the presence of mannoproteins at a concentration of 1 and 0.5 $g.L^{-1}$. As the results at different mannoproteins concentrations were very alike, only those obtained at 1 $g.L^{-1}$ are detailed thereafter. In the first series of experiments, mannoproteins and tannins were mixed first, and the BSA was added to this solution after 1 hour. The results obtained are summarized (**Figure 1**) and compared to those of the controls (BSA+SWT). In the second series of experiments, mannoproteins and BSA were mixed first and tannins were added after 1 hour. Very similar results were obtained when adding either BSA or SWT last (**Figure 1**). Mannoprotein-tannin (MP+SWT) and mannoprotein-BSA (MP+BSA) mixtures (without the addition of the third component) remained stable during the whole experiment. If any interaction between mannoproteins and BSA happened, it did not result in the formation of aggregates that could be observed by DLS. Likewise, mannoproteins and red wine tannins formed stable colloidal mixtures, with an average D_{hS} of colloids close to that of the mannoprotein alone.

Depending on the MP, very different behaviors were observed when BSA was added. MP-Com did not strongly modify Tannin-BSA aggregation kinetic nor the average aggregate size. The latter was only slightly smaller. By contrast, MP-WT and MP-Mnn4 had a remarkable effect on tannin-BSA aggregation. Scattered-Intensity (I_S) profiles for both MPs were very similar to that of control samples although higher and remained stable for one hour, while the average aggregate size (D_{hS}) quickly reached a plateau value around 500 nm that did not evolve during the experiment duration (1 h). Higher I_S values when D_{hS} is lower than control samples

may seem contradictory – given the dependence of scattered light intensity on the particle size (proportional to the particle diameter to the 6th power) – but can be explained if the particle concentration in samples with MPs was much higher. In addition, the intensity of the light scattered by mannoproteins themselves must be accounted for (around 10 000 kcps).

The results observed with MP-Mnn2 after BSA addition were intermediate between those of the MP-Com and those of the MP-WT and Mnn4. Large aggregates were quickly formed within the first 10 minutes of interaction, as for MP-Com. However, aggregate size remained stable (1 to 1.5 µm) and smaller than that observed with the control during most of the experiment, as with MP-WT and Mnn4. The decay of I_S started sooner than with the other MPs (around 34 min), indicating that the colloids formed in the presence of MP-Mnn2 become unstable earlier than those formed with the other MPs.

After 24 hours, a visible precipitate had formed in all BSA+SWT and MP+BSA+SWT samples. Samples were centrifuged after 48 hours and the amount of tannins within the precipitates was quantified by absorbance measurements of the supernatant after applying a proper dilution-factor (**Table 1**). Similar values were obtained in controls and MP samples: about 23 – 24 % of the tannins were precipitated. This indicated that mannoproteins may interfere with the aggregation process but do not prevent it. On average, fewer tannins were precipitated in MP/BSA+SWT samples than in MP/SWT+BSA ones, although this difference was not statistically significant.

Supernatant and precipitates were also analyzed through HPSEC-DAD to obtain the size distribution profiles of tannins (**Supplementary data, Figure S3**). The highest-size tannins were preferentially involved in interactions with BSA and precipitation, in agreement with the literature data (Frazier, Papadopoulou, Mueller-Harvey, Kissoon, & Green, 2003; McRae et al., 2010). No difference existed between the molecular size-distribution profiles of

MP/BSA+SWT samples and that of MP/SWT+BSA ones (results not shown). Results confirmed those obtained through absorbance measurements (**Table 1**).

In control samples, there were three distinctive stages in the aggregation process: first the interaction between BSA and SWT molecules and the immediate formation of small aggregates (primary aggregates). At high tannin/protein molar ratios such as those used in the present study, aggregation is attributed to the coating of BSA by SWT molecules, leading to the formation of poorly soluble complexes that aggregate (Siebert, 2006). In our measurements, this stage corresponds to the sharp increase in scattered intensity observed during the first minutes of interaction. In the second stage, the enlarged aggregation of these primary aggregates induces a quick increase in particle size (D_{hS} increase with stable I_S values). This led to particles whose size was too large to be kept in suspension and this resulted in the gradual decrease in I_S and a phase separation observed after 24 hours.

Present results indicated that mannoproteins do not strongly interfere with the initial interaction between BSA and red wine tannins. This is consistent with the much higher affinity evidenced in the literature by ITC for the interactions between tannins and BSA by comparison to those between tannins and mannoproteins (Frazier, Papadopoulou, & Green, 2006; Mekoue Nguela et al., 2016). However, mannoproteins, depending on the structure of their polysaccharide part, were more or less able to interfere in the second step, that is the quick enlarged aggregation observed in the controls. This could be related to a) interactions between MPs and BSA or between MPs and tannins, even at low affinities, that delayed BSA/tannins interactions; b) interactions between mannoproteins and BSA/tannin aggregates (mannoprotein adsorption on tannin/BSA aggregates) that slow down aggregate growth. The first hypothesis does not comply with the results: whatever the order of addition (MP+SWT solution then added with BSA or MP+BSA solution then added with SWT), similar DLS profiles and % of precipitated tannins were obtained. In addition, this hypothesis is not consistent with the immediate increase in

intensity observed and the evolution of the aggregate diameter. It is more likely that mannoproteins have a more or less important impact on initial aggregate growth depending on their ability to adsorb on these aggregates and to “stabilize” them in the short term by the formation of an external hydrophilic polysaccharide layer (steric repulsion) (**Figure 2**). The differences observed between the four mannoprotein fractions can be explained by the differences that exist in the structure of their polysaccharide moiety. MP-Com, which presents a more branched and dense structure than the others, was not able to adsorb on tannin-BSA aggregates through their protein part. This adsorption occurred for the three other MPs. Higher effects were observed for MP-WT and MP-Mnn4 by comparison to MP-Mnn2. Thus, the absence of →2,6)-Man-(1→ branching linkages on the backbone of the N-glycosylation reduces the steric hindrance promoted by the polysaccharide part that delays BSA/SWT particle growth. In any case, if this effect is visible during the first hour of interaction, this adsorption must be reversible because it does not result in long-term stabilization.

Few studies have also taken interest in mannoproteins capacity to modulate astringency through the aggregates formed during tannin-protein interactions, and most of them are not entirely comparable with the methodology applied in this work. Wang et al. evaluated the interactions between BSA and three different wine polyphenol fractions: i) phenolic acids, ii) monomeric and oligomeric polyphenols, and iii) polymeric polyphenols. The DLS measurements did not take into account the time dependence of the size and quantity of the particles formed. They were performed in samples that were centrifuged analyzing only particles that remained in suspension after the aggregation process. Corroborating with our results, interactions were the most intense with polyphenolic fractions of the largest aDP (largest particles remaining in suspension, 1 500 nm). The addition of three different commercial preparations of mannoproteins before BSA addition reduced particle size of the aggregates that remained in suspension (between 300 and 600 nm). However, no quantification of the polyphenol content

that precipitated was performed to evaluate if MPs induced the precipitation of larger aggregates or if smaller and more stable aggregates were formed.

3.2 Co-pigmentation between Mal3glc and Mannoproteins

Absorbance spectra recorded during the titrations of MP solutions with Mal3glc are shown in **Figure 3** and compared with those of the control. The absorbance increment at 525 nm is represented for the four MPs as a function of the Mal3glc concentration in **Figure 3E**. In the control samples, a linear increase of A_{525} with the Mal3glc concentration was observed, in accordance with the Beer-Lambert law. This indicated that Mal3glc did not self-associate at the concentrations reached during titration in agreement with previous studies (González-Manzano, Santos-Buelga, Dueñas, Rivas-Gonzalo, & Escribano-Bailón, 2008; Houbiers, Lima, Maçanita, & Santos, 1998). After each addition, the increase in Mal3glc concentration in control samples led to an increase of the absorbance at 525 nm that differed from those observed with the MP samples. Although very small compared to those of phenolic co-pigments (R. Brouillard, Mazza, Saad, Albrecht-Gary, & Cheminat, 1989; Lambert, Asenstorfer, Williamson, Iland, & Jones, 2011; Malaj, Simone, Quartarolo, & Russo, 2013), a hyperchromic effect that increased with the concentration in Mal3glc was observed with MP-WT and MP-Mnn2. MP-Com and MP-Mnn4 did not induce the same hyperchromic effect and the increases observed during the last additions were within the range of the experimental error. Indeed, the absorbance variation caused by the hyperchromic effect of MPs was weaker than that caused by the variation of Mal3glc concentration.

To confirm these results, absorbance spectra of Mal3glc were also measured in the presence of higher mannoprotein concentrations (1 and 2 $g.L^{-1}$). Results confirmed the lack of effect of MP-Com and indicated a slight hyperchromic effect with the three other mannoproteins (**Table 2**). The increases in absorbance observed at the highest MP concentrations in solution (2 $g.L^{-1}$) were 2.2, 7.2, and 1.5 % for MP-WT, MP-Mnn2, and MP-Mnn4, respectively.

Some polysaccharides have been described as non-phenolic copigments of anthocyanins that cause weak hyperchromic effects but no bathochromic or hypsochromic shifts like phenolic copigments such as flavonols and phenolic acids (Maier, Fromm, Schieber, Kammerer, & Carle, 2009; Mazzaracchio, Pifferi, Kindt, Munyaneza, & Barbiroli, 2004; Trouillas et al., 2016). Co-pigmentation effect is mainly attributed to the presence of galacturonic acid residues in the HG chains and their pH-dependent negative charge: electrostatic interactions between carboxylic anions and flavylium cations is then the triggering event for anthocyanin binding to the polysaccharides (Buchweitz, Speth, Kammerer, & Carle, 2013; Fernandes et al., 2020). These bonds shift the equilibrium between colored flavylium (A+) and colorless hydrated forms (AH) for non-interacting anthocyanins at the pH considered, causing an increase of the A+ forms in the solution (Raymond Brouillard & Dubois, 1977). The affinity of pectins for anthocyanins and their impact on absorbance is dependent on their structure and composition. Pectins with low methyl-esterified HG and/or less branched regions were described as having higher affinities for Mal3glc and cyanidin-3-*O*-glucoside (Fernandes et al., 2016, 2020, 2021; Maier et al., 2009; Mazzaracchio et al., 2004).

Although performed in different media in terms of ethanol content and ionic strength, results obtained here with mannoproteins can be compared to those reported in the literature for different pectic polysaccharides. Absorbance increments were much lower than those obtained for different pectins with low esterification degree and high proportions of uronic acids (increase in absorbance between 19 and 40%, and up to 200% in some cases). This hyperchromic effect was strongly reduced by the esterification of the galacturonic acid residues and by the presence of neutral sugar lateral chains. The net charge of the mannoproteins results from the presence of the strong acidic phosphate groups associated with mannosyl-phosphate residues, and the presence of basic and acidic amino acid residues in their protein part. The four mannoprotein fractions studied have the same amino acid composition of their protein part,

which represents from 3.6 to 5.4 % w/w of the whole mannoproteins. By contrast, the structures of their polysaccharide part differed in terms of branching degree and mannosyl-phosphorylation, which is responsible for the presence of a negative charge on polysaccharide chains at pH 3.5. The net charge of the four mannoprotein fractions is very small at pH 3.5 (Assunção Bicca et al., 2022 and **Supplementary data Table S1**). If the co-pigmentation effect between anthocyanins and polysaccharides is mainly driven by electrostatic interactions, it explains their very low impact on color compared to certain pectic polysaccharides.

Although this net charge was small at the studied pH, MPs could be ranked as a function of their negative charge density as follows: MP-Com>MP-WT>=MP-Mnn2>>MP-Mnn4 (Assunção Bicca et al., 2022). Results obtained with WP-WT, MP-Mnn2, and MP-Mnn4 (devoid of mannosyl-phosphate groups) are consistent with a hyperchromic effect of MPs related to electrostatic interactions. The slightly higher hyperchromic shift found for Mnn2 could be related to higher accessibility to the interaction sites (no branching of the N-glycosylated chains). In contrast, the low affinity between MP-Com and Mal3glc could be explained by its more branched and compact structure, which hinders anthocyanin accessibility to interaction sites although MP-Com is the most negatively charged mannoproteins at the pH considered.

3.3 Mannoprotein impact on malvidin-3-*O*-glucoside copigmentation with quercetin-3-*O*-glucoside

In this work, the objective was to evaluate the impact of mannoproteins on the co-pigmentation between anthocyanins and quercetin-3-*O*-glucoside (Qrc3glc). To this end, absorbance spectra were recorded during the progressive addition of Qrc3glc to Mal3glc + MP solutions (**Figure 4**). Due to the low availability of the studied mannoproteins, this method was applied with a much lower variation of the co-pigment (Qrc3glc) concentrations. At pH 3.5, the maximum absorbance for Mal3glc alone was observed at 525 nm. However, a bathochromic

shift was observed as Qrc3glc concentration in the samples increased. Whatever the considered MP, the addition of Qrc3glc provoked the same shift of the maximum wavelength as that observed in control samples. This indicated that MPs did not interfere in the co-pigmentation between Mal3glc and Qrc3glc. On the other hand, the intensity of the hyperchromic shift was greater in the presence of MP-Mnn2 and MP-WT, which increased with increasing Qrc3glc content. No substantial differences were noticed for MP-Com and MP-Mnn4. This suggests that interactions between MPs and Mal3glc also occur in the presence of Qrc3glc at the tested concentrations and that there is a synergistic effect between the two copigments.

4 Conclusion

In this study, we elucidated the capacity of mannoproteins to impact the colloidal growth of aggregates formed by the protein-tannins interactions and the importance of the polysaccharide moiety to it. Although the latter does not play a major role in the interactions between mannoproteins and tannins, structural aspects of the polysaccharide moiety were essential to the stability of the colloidal complexes formed. In particular, the compactness of the polysaccharide moiety seems to have a double-edged effect:

i) denser macromolecules, like MP-Com and the high branching degree of its protein part, promoted steric-hindrance and low accessibility of interaction sites that prevent its adsorption on tannin/BSA aggregates;

ii) less dense and more elongated structures, such as MP-Mnn2, produced less stable ternary aggregates.

Two different mechanisms may explain the lower efficiency of Mnn2 when compared to MP-WT and Mnn4: insufficient steric hindrance to counteract as effectively the enlarged aggregation of tannin/BSA primary aggregates and/or a greater propensity to bridge different aggregates. However, the outcomes obtained are not directly relatable to astringency. To this

end, a more specific test is needed (Boulet et al., 2016), in which shorter periods of interactions are considered, compatible with the tasting, and that relates protein stability to astringency. To bring progressively the experimental conditions to the real wine-tasting conditions, it would also be interesting to evaluate mannoproteins impact on tannin interactions with salivary proteins.

This study also evidenced the existence of interactions between mannoproteins and malvidin-3-*O*-glucoside, which depends on the polysaccharide structure. The different behaviors of the studied mannoproteins revealed the impact of the net negative charge of mannosyl-phosphate groups as well as their accessibility within the polysaccharide structure. With the studied mannoproteins, there are only a few interactions (few sites per molecule) and therefore they have little impact on the color of Mal3glc. Further studies will be needed to evaluate the interactions between mannoproteins and other wine pigments, such as acylated anthocyanins and polymeric pigments.

5 References

Assunção Bicca, S., Poncet-Legrand, C., Williams, P., Mekoue Nguela, J., Doco, T., & Vernhet, A. (2022). Structural characteristics of Saccharomyces cerevisiae mannoproteins: Impact of their polysaccharide part. *Carbohydrate Polymers*, *277*(September 2021), 118758. https://doi.org/10.1016/j.carbpol.2021.118758

Bate-Smith, E. C. (1973). Haemanalysis of tannins: The concept of relative astringency. *Phytochemistry*, *12*(4), 907–912. https://doi.org/10.1016/0031-9422(73)80701-0

Boulet, J.-C., Trarieux, C., Souquet, J.-M., Ducasse, M.-A., Caillé, S., Samson, A., … Cheynier, V. (2016). Models based on ultraviolet spectroscopy, polyphenols, oligosaccharides and polysaccharides for prediction of wine astringency. *Food Chemistry*, *190*, 357–363. https://doi.org/10.1016/j.foodchem.2015.05.062

Brandão, E., Silva, M. S., García-Estévez, I., Williams, P., Mateus, N., Doco, T., … Soares, S. (2017). The role of wine polysaccharides on salivary protein-tannin interaction: A molecular approach. *Carbohydrate Polymers*, *177*(May), 77–85. https://doi.org/10.1016/j.carbpol.2017.08.075

Brouillard, R., Mazza, G., Saad, Z., Albrecht-Gary, A. M., & Cheminat, A. (1989). The Copigmentation Reaction of Anthocyanins: A Microprobe for the Structural Study of Aqueous Solutions. *Journal of the American Chemical Society*, *111*(7), 2604–2610. https://doi.org/10.1021/ja00189a039

Brouillard, Raymond, & Dubois, J. E. (1977). Mechanism of the Structural Transformations of Anthocyanins in Acidic Media. *Journal of the American Chemical Society*, *99*(5), 1359–1364. https://doi.org/10.1021/ja00447a012

Buchweitz, M., Speth, M., Kammerer, D. R., & Carle, R. (2013). Impact of pectin type on the storage stability of black currant (Ribes nigrum L.) anthocyanins in pectic model solutions.

Food Chemistry, *139*(1–4), 1168–1178. https://doi.org/10.1016/j.foodchem.2013.02.005

Carvalho, E., Póvoas, M. J., Mateus, N., & De Freitas, V. (2006). Application of flow nephelometry to the analysis of the influence of carbohydrates on protein-tannin interactions. *Journal of the Science of Food and Agriculture*, *86*(6), 891–896. https://doi.org/10.1002/jsfa.2430

Cheynier, V. (2012). Phenolic compounds: from plants to foods. *Phytochemistry Reviews*, *11*(2–3), 153–177. https://doi.org/10.1007/s11101-012-9242-8

Cheynier, V., Dueñas-Paton, M., Salas, E., Maury, C., Souquet, J. M., Sarni-Manchado, P., & Fulcrand, H. (2006). Structure and properties of wine pigments and tannins. *American Journal of Enology and Viticulture*, *57*(3), 298–305.

De Freitas, V., & Mateus, N. (2011). Formation of pyranoanthocyanins in red wines: A new and diverse class of anthocyanin derivatives. *Analytical and Bioanalytical Chemistry*, *401*(5), 1467–1477. https://doi.org/10.1007/s00216-010-4479-9

Escot, S., Feuillat, M., Dulau, L., & Charpentier, C. (2001). Release of polysaccharides by yeasts and the influence of released polysaccharides on colour stability and wine astringency. *Australian Journal of Grape and Wine Research*, *7*(3), 153–159. https://doi.org/10.1111/j.1755-0238.2001.tb00204.x

Fernandes, A., Brás, N. F., Oliveira, J., Mateus, N., & De Freitas, V. (2016). Impact of a pectic polysaccharide on oenin copigmentation mechanism. *Food Chemistry*, *209*, 17–26. https://doi.org/10.1016/j.foodchem.2016.04.018

Fernandes, A., Oliveira, J., Fonseca, F., Ferreira-da-Silva, F., Mateus, N., Vincken, J. P., & de Freitas, V. (2020). Molecular binding between anthocyanins and pectic polysaccharides – Unveiling the role of pectic polysaccharides structure. *Food Hydrocolloids*, *102*. https://doi.org/10.1016/j.foodhyd.2019.105625

Fernandes, A., Raposo, F., Evtuguin, D. V., Fonseca, F., Ferreira-da-Silva, F., Mateus, N., …

de Freitas, V. (2021). Grape pectic polysaccharides stabilization of anthocyanins red colour: Mechanistic insights. *Carbohydrate Polymers*, *255*(November 2020). https://doi.org/10.1016/j.carbpol.2020.117432

Frazier, R. A., Papadopoulou, A., & Green, R. J. (2006). Isothermal titration calorimetry study of epicatechin binding to serum albumin. *Journal of Pharmaceutical and Biomedical Analysis*, *41*(5), 1602–1605. https://doi.org/10.1016/j.jpba.2006.02.004

Frazier, R. A., Papadopoulou, A., Mueller-Harvey, I., Kissoon, D., & Green, R. J. (2003). Probing protein-tannin interactions by isothermal titration microcalorimetry. *Journal of Agricultural and Food Chemistry*, *51*(18), 5189–5195. https://doi.org/10.1021/jf021179v

Fulcrand, H., Dueñas, M., Salas, E., & Cheynier, V. (2006). Phenolic reactions during winemaking and aging. *American Journal of Enology and Viticulture*, *57*(3), 289–297.

Gonçalves, F. J., Fernandes, P. A. R., Rocha, S. M., Coimbra, M. A., Wessel, D. F., & Cardoso, S. M. (2018). Interaction of wine mannoproteins and arabinogalactans with anthocyanins. *Food Chemistry*, *243*(February 2017), 1–10. https://doi.org/10.1016/j.foodchem.2017.09.097

Gonçalves, F. J., Rocha, S. M., & Coimbra, M. A. (2012). Study of the retention capacity of anthocyanins by wine polymeric material. *Food Chemistry*, *134*(2), 957–963. https://doi.org/10.1016/j.foodchem.2012.02.214

González-Manzano, S., Santos-Buelga, C., Dueñas, M., Rivas-Gonzalo, J. C., & Escribano-Bailón, T. (2008). Colour implications of self-association processes of wine anthocyanins. *European Food Research and Technology*, *226*(3), 483–490. https://doi.org/10.1007/s00217-007-0560-9

González-Muñoz, B., Garrido-Vargas, F., Pavez, C., Osorio, F., Chen, J., Bordeu, E., … Brossard, N. (2022). Wine astringency: more than just tannin–protein interactions. *Journal of the Science of Food and Agriculture*, *102*(5), 1771–1781.

https://doi.org/10.1002/jsfa.11672

Guadalupe, Z., Martínez, L., & Ayestarán, B. (2010). Yeast mannoproteins in red winemaking: Effect on polysaccharide, polyphenolic, and color composition. *American Journal of Enology and Viticulture*, *61*(2), 191–200.

Harbertson, J. F., Kilmister, R. L., Kelm, M. A., & Downey, M. O. (2014). Impact of condensed tannin size as individual and mixed polymers on bovine serum albumin precipitation. *Food Chemistry*, *160*, 16–21. https://doi.org/10.1016/j.foodchem.2014.03.026

Houbiers, C., Lima, J. C., Maçanita, A. L., & Santos, H. (1998). Color stabilization of malvidin 3-glucoside: Self-aggregation of the flavylium cation and copigmentation with the Z-chalcone form. *Journal of Physical Chemistry B*, *102*(18), 3578–3585. https://doi.org/10.1021/jp972320j

Kennedy, J. A., & Jones, G. P. (2001). Analysis of proanthocyanidin cleavage products following acid-catalysis in the presence of excess phloroglucinol. *Journal of Agricultural and Food Chemistry*, *49*(4), 1740–1746. https://doi.org/10.1021/jf001030o

Lambert, S. G., Asenstorfer, R. E., Williamson, N. M., Iland, P. G., & Jones, G. P. (2011). Copigmentation between malvidin-3-glucoside and some wine constituents and its importance to colour expression in red wine. *Food Chemistry*, *125*(1), 106–115. https://doi.org/10.1016/j.foodchem.2010.08.045

Lin, Z., Fischer, J., & Wicker, L. (2016). Intermolecular binding of blueberry pectin-rich fractions and anthocyanin. *Food Chemistry*, *194*, 986–993. https://doi.org/10.1016/j.foodchem.2015.08.113

Maier, T., Fromm, M., Schieber, A., Kammerer, D. R., & Carle, R. (2009). Process and storage stability of anthocyanins and non-anthocyanin phenolics in pectin and gelatin gels enriched with grape pomace extracts. *European Food Research and Technology*, *229*(6), 949–960. https://doi.org/10.1007/s00217-009-1134-9

Malaj, N., Simone, B. C. De, Quartarolo, A. D., & Russo, N. (2013). Spectrophotometric study of the copigmentation of malvidin 3-O-glucoside with p-coumaric, vanillic and syringic acids. *Food Chemistry*, *141*(4), 3614–3620. https://doi.org/10.1016/j.foodchem.2013.06.017

Manjón, E., Recio-Torrado, A., Ramos-Pineda, A. M., García-Estévez, I., & Escribano-Bailón, M. T. (2021). Effect of different yeast mannoproteins on the interaction between wine flavanols and salivary proteins. *Food Research International*, *143*(February). https://doi.org/10.1016/j.foodres.2021.110279

Mazzaracchio, P., Pifferi, P., Kindt, M., Munyaneza, A., & Barbiroli, G. (2004). Interactions between anthocyanins and organic food molecules in model systems. *International Journal of Food Science and Technology*, *39*(1), 53–59. https://doi.org/10.1111/j.1365-2621.2004.00747.x

McRae, J. M., Falconer, R. J., & Kennedy, J. A. (2010). Thermodynamics of grape and wine tannin interaction with polyproline: Implications for red wine astringency. *Journal of Agricultural and Food Chemistry*, *58*(23), 12510–12518. https://doi.org/10.1021/jf1030967

Mekoue Nguela, J., Poncet-Legrand, C., Sieczkowski, N., & Vernhet, A. (2016). Interactions of grape tannins and wine polyphenols with a yeast protein extract, mannoproteins and β-glucan. *Food Chemistry*, *210*, 671–682. https://doi.org/10.1016/j.foodchem.2016.04.050

Oyón-Ardoiz, M., Manjón, E., Escribano-Bailón, M. T., & García-Estévez, I. (2022). Effect of mannoproteins from different oenological yeast on pigment composition and color stability of red wine. *Lwt*, *172*(November). https://doi.org/10.1016/j.lwt.2022.114219

Padayachee, A., Netzel, G., Netzel, M., Day, L., Zabaras, D., Mikkelsen, D., & Gidley, M. J. (2012). Binding of polyphenols to plant cell wall analogues - Part 1: Anthocyanins. *Food Chemistry*, *134*(1), 155–161. https://doi.org/10.1016/j.foodchem.2012.02.082

Quijada-Morín, N., Williams, P., Rivas-Gonzalo, J. C., Doco, T., & Escribano-Bailón, M. T. (2014). Polyphenolic, polysaccharide and oligosaccharide composition of Tempranillo red wines and their relationship with the perceived astringency. *Food Chemistry*, *154*, 44–51. https://doi.org/10.1016/j.foodchem.2013.12.101

Rinaldi, A., Coppola, M., & Moio, L. (2019). Aging of Aglianico and Sangiovese wine on mannoproteins: Effect on astringency and colour. *Lwt*, *105*(February), 233–241. https://doi.org/10.1016/j.lwt.2019.02.034

Siebert, K. J. (2006). Haze formation in beverages. *LWT - Food Science and Technology*, *39*(9), 987–994. https://doi.org/10.1016/j.lwt.2006.02.012

Soares, S., Mateus, N., & de Freitas, V. (2012). Carbohydrates Inhibit Salivary Proteins Precipitation by Condensed Tannins. *Journal of Agricultural and Food Chemistry*, *60*(15), 3966–3972. https://doi.org/10.1021/jf3002747

Trouillas, P., Sancho-García, J. C., De Freitas, V., Gierschner, J., Otyepka, M., & Dangles, O. (2016). Stabilizing and Modulating Color by Copigmentation: Insights from Theory and Experiment. *Chemical Reviews*, *116*(9), 4937–4982. https://doi.org/10.1021/acs.chemrev.5b00507

Vidal, S., Francis, L., Guyot, S., Marnet, N., Kwiatkowski, M., Gawel, R., … Waters, E. J. (2003). The mouth-feel properties of grape and apple proanthocyanidins in a wine-like medium. *Journal of the Science of Food and Agriculture*, *83*(6), 564–573. https://doi.org/10.1002/jsfa.1394

Wang, S., Wang, X., Zhao, P., Ma, Z., Zhao, Q., Cao, X., … Du, G. (2021). Mannoproteins interfering wine astringency by modulating the reaction between phenolic fractions and protein in a model wine system. *Lwt*, *152*(620), 112217. https://doi.org/10.1016/j.lwt.2021.112217

Tables

Table 1: TPI measurements of samples supernatants after 48 h expressed in SWT (Syrah Wine Tannins) percentage that remained in solution by comparison to control samples (SWT 0.2 $g.L^{-1}$). MP/SWT+BSA stands for samples where BSA was added last while MP/BSA+SWT stands for samples where SWT were added last. 0.5MP/SWT+BSA regards samples with 0.5 $g.L^{-1}$ mannoprotein concentration. ANOVA analysis (right side) were performed using SNK test p=0.05.

	Abs_{280}			% SWT supernatant			
SWT	0,247	±	0,002	100			
SWT+BSA	0,190	±	0,001	76,8	±	0,4	
MP/SWT+BSA							
MP-Com	0,188	±	0,004	75,9	±	1,4	a
MP-WT	0,192	±	0,003	77,6	±	1,1	a
MP-Mnn2	0,185	±	0,004	74,8	±	1,5	a
MP-Mnn4	0,192	±	0,004	77,5	±	1,7	a
MP/BSA+SWT							
MP-Com	0,194	±	0,003	78,6	±	1,0	a
MP-WT	0,194	±	0,004	78,3	±	1,7	a
MP-Mnn2	0,190	±	0,001	76,7	±	0,5	a
MP-Mnn4	0,196	±	0,002	79,2	±	0,8	a
0.5MP/SWT+BSA							
MP-Com	0,188	±	0,001	77,8	±	0,6	a
MP-WT	0,188	±	0,002	75,9	±	0,8	a
MP-Mnn2	0,190	±	0,003	77,0	±	1,2	a
MP-Mnn4	0,187	±	0,004	75,7	±	1,6	a

Table 2: Relative absorbance shifts 100*((Abs-Abs0)/Abs0) observed for the different MPs at different mass ratios.

	1:20	1:40
MP-Com	0.7 ± 0.2	0.2 ± 0.5
MP-WT	1.2 ± 0.2	2.3 ± 0.5
MP-Mnn2	3.0 ± 0.4	7.2 ± 1.9
MP-Mnn4	0.8 ± 0.6	1.5 ± 0.6

Figure captions

Figure 1: Evolution of the hydrodynamic diameter D_{hS} (on the left) and Scattered-Light Intensity I_S (on the right) of samples over time. In Red (1): MP-Com, Green (2): MP-WT, Blue (3): MP-Mnn2, Violet (4): MP-Mnn4. Black circles: SWT + BSA. Squares: blank samples (MP+SWT solutions). MPs alone and MP+BSA solutions, which were very similar to the MP+SWT solutions, were not plotted here for the sake of clarity. Triangles: MP+SWT solutions added with BSA; stars: MP+BSA solutions added with SWT. I_S values at time zero were theoretically calculated as the sum of the I_S from blank solutions of MP, SWT, and BSA at their respective concentrations in the samples, while only the D_{hS} of MPs were taking in consideration due to their much higher size and concentration compared to SWT and BSA.

Figure 2: Schematic illustration of BSA/Tannins aggregation process and the effect of mannoproteins into slowing down particle size increase.

Figure 3: Absorbance spectra of the MP solutions during the progressive addition of Malvidin-3-*O*-Glucoside (colored spectra) by comparison to that of the control sample (black spectra, without MPs). Spectra in red (A): MP-Com; spectra in green(B): MP-WT, blue (C): MP-Mnn2, spectra in violet (D): MP-Mnn4. Figure E: Absorbance shift (ΔAbs) at 525 nm in the presence of mannoproteins (Abs) by comparison to a control (Abs^0) during the progressive addition of Mal3glc in a model wine. Results represent the mean of 3 experiments.

Figure 4: Absorbance spectra of (MP+Mal3glc) solutions titrated with quercetin-3-*O*-glucoside. MP-Com (Red), MP-WT (Green), MP-Mnn2 (Blue), and MP-Mnn4 (Violet). Spectra in black full-lines are from the titration of Mal3glc alone with the copigment.

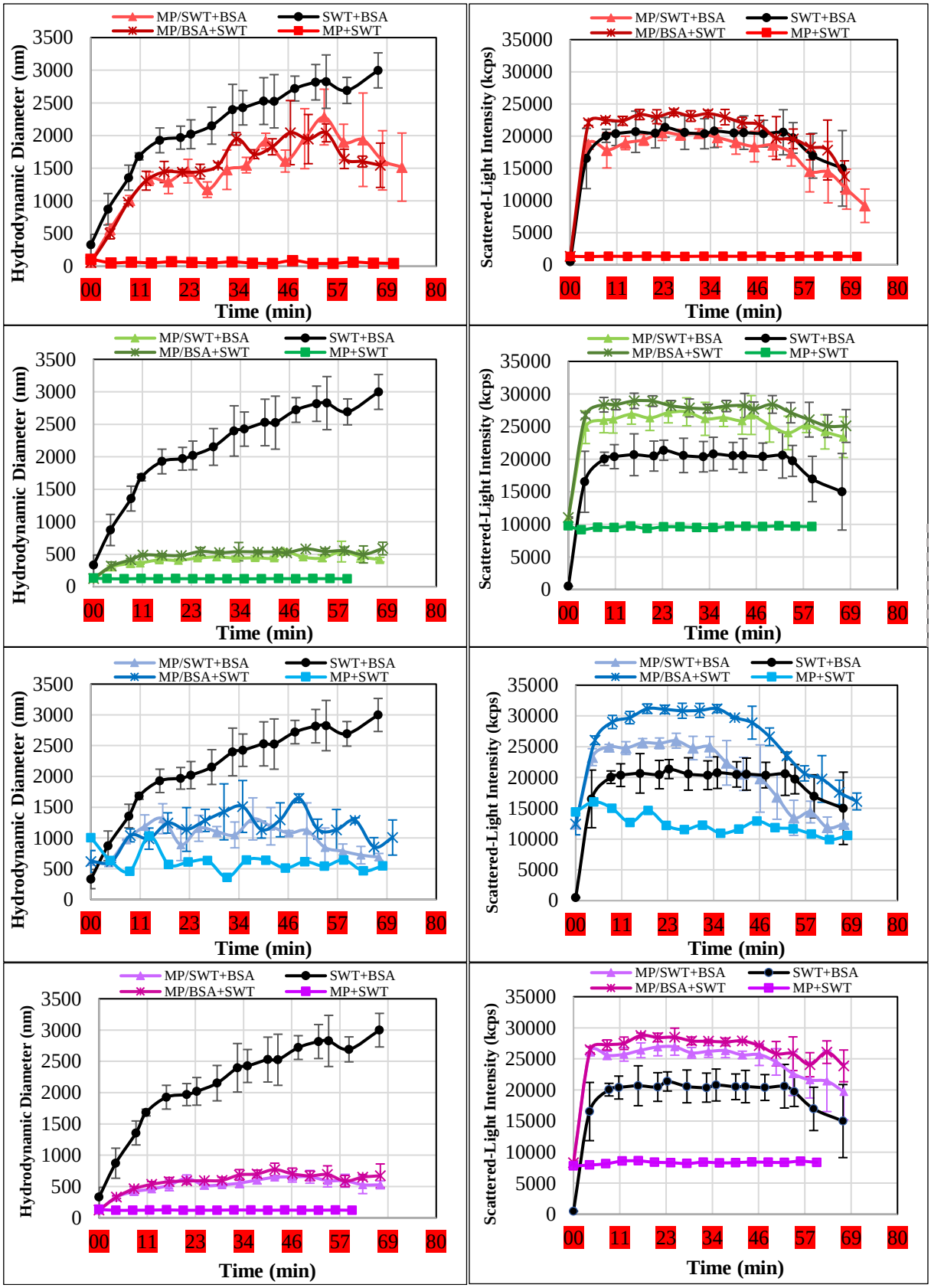

Assunção Bicca *et al.*, **Figure 1**

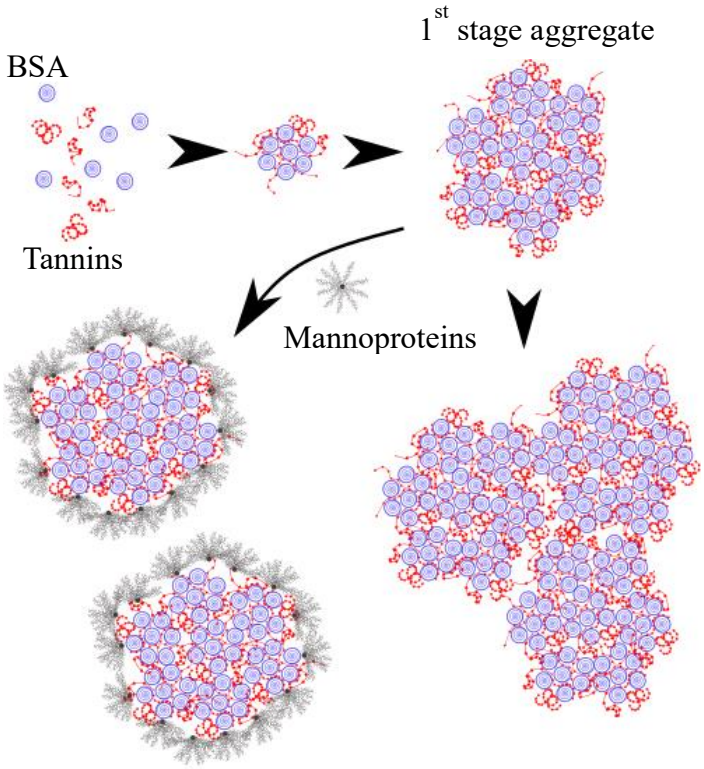

Assunção Bicca *et al.*, **Figure 2**

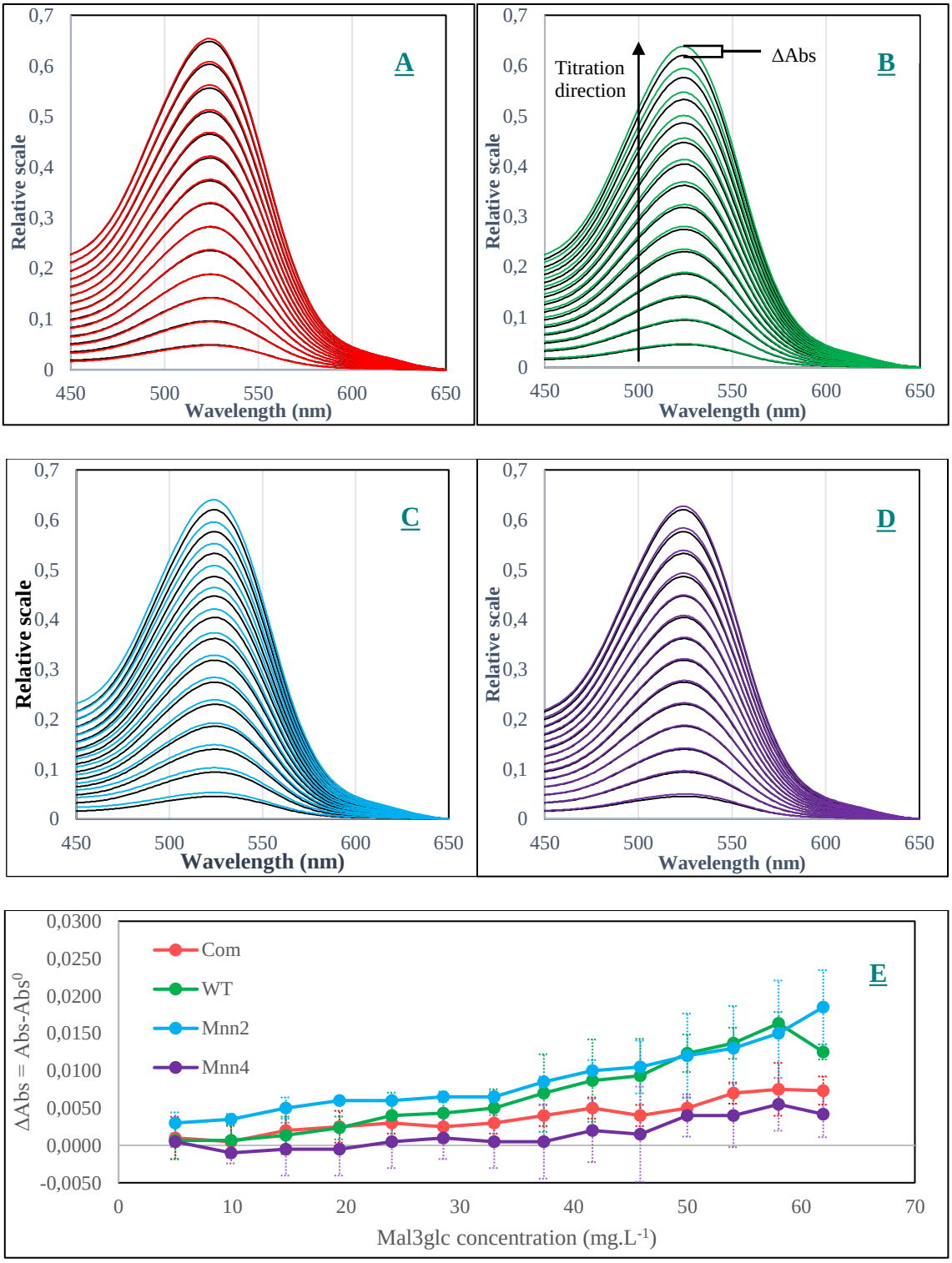

Assunção Bicca *et al.*, **Figure 3**

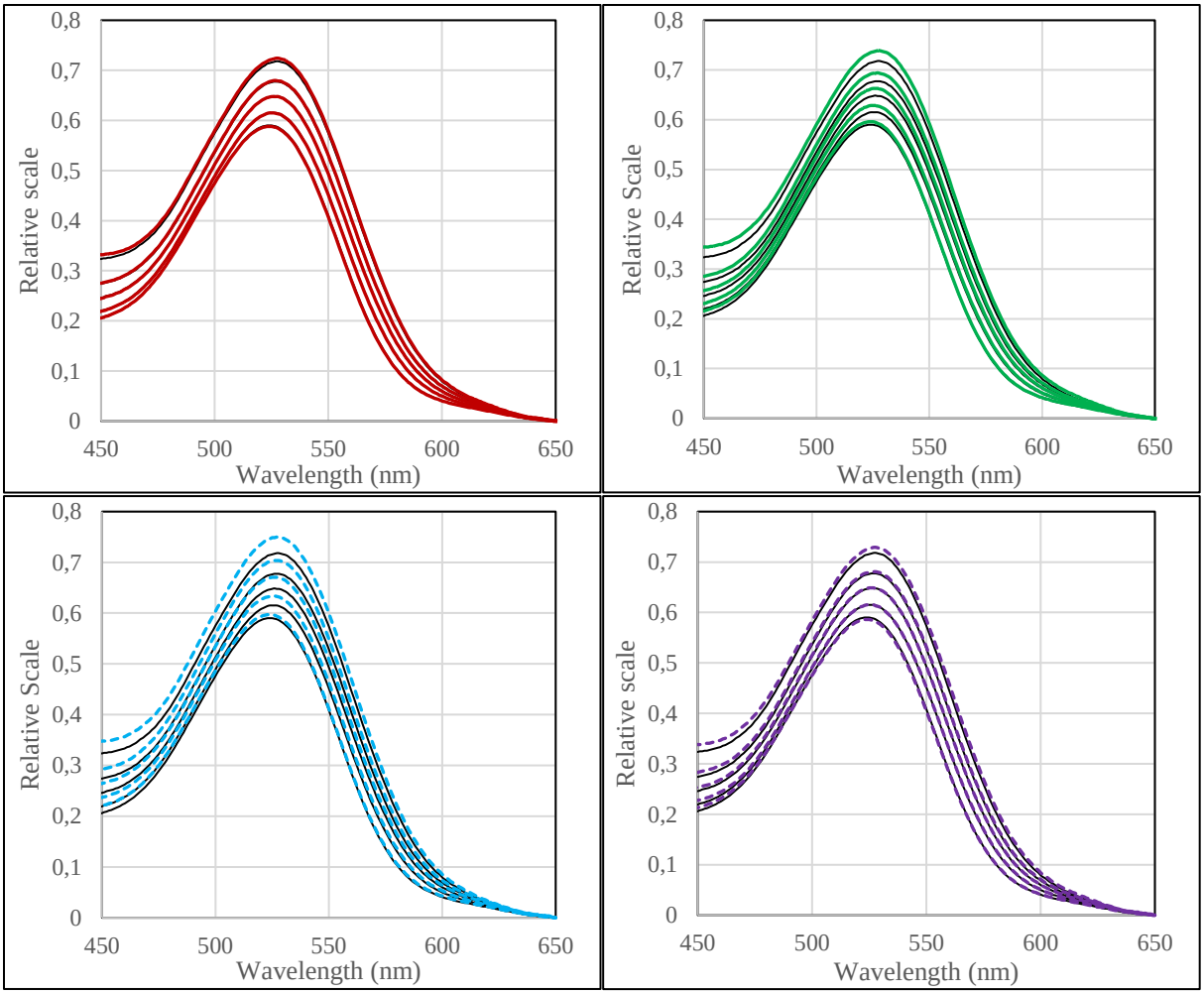

Assunção Bicca *et al.*, **Figure 4**